




Article

Biochemical and Proteomic Changes in the Roots of M4 Grapevine Rootstock in Response to Nitrate Availability

Bhakti Prinsi , Chiara Muratore  and Luca Espen 

Department of Agricultural and Environmental Sciences—Production, Landscape, Agroenergy (DiSAA),
Università degli Studi di Milano, I-20133 Milano, Italy; bhakti.prinsi@unimi.it (B.P.);
chiara.muratore@unimi.it (C.M.)

* Correspondence: luca.espen@unimi.it; Tel.: +39-02-503-16610

Abstract: In agricultural soils, nitrate (NO_3^-) is the major nitrogen (N) nutrient for plants, but few studies have analyzed molecular and biochemical responses involved in its acquisition by grapevine roots. In viticulture, considering grafting, NO_3^- acquisition is strictly dependent on rootstock. To improve the knowledge about N nutrition in grapevine, this study analyzed biochemical and proteomic changes induced by, NO_3^- availability, in a hydroponic system, in the roots of M4, a recently selected grapevine rootstock. The evaluation of biochemical parameters, such as NO_3^- , sugar and amino acid contents in roots, and the abundance of nitrate reductase, allowed us to define the time course of the metabolic adaptations to NO_3^- supply. On the basis of these results, the proteomic analysis was conducted by comparing the root profiles in N-starved plants and after 30 h of NO_3^- resupply. The analysis quantified 461 proteins, 26% of which differed in abundance between conditions. Overall, this approach highlighted, together with an increased N assimilatory metabolism, a concomitant rise in the oxidative pentose phosphate pathway and glycolysis, needed to fulfill the redox power and carbon skeleton demands, respectively. Moreover, a wide modulation of protein and amino acid metabolisms and changes of proteins involved in root development were observed. Finally, some results open new questions about the importance of redox-related post-translational modifications and of NO_3^- availability in modulating the dialog between root and rhizosphere.

Keywords: *Vitis*; mineral plant nutrition; perennial crop; nitrate; root growth



Citation: Prinsi, B.; Muratore, C.; Espen, L. Biochemical and Proteomic Changes in the Roots of M4 Grapevine Rootstock in Response to Nitrate Availability. *Plants* **2021**, *10*, 792. <https://doi.org/10.3390/plants10040792>

Academic Editor: Klára Kosová

Received: 13 March 2021

Accepted: 15 April 2021

Published: 17 April 2021

Publisher's Note: MDPI stays neutral with regard to jurisdictional claims in published maps and institutional affiliations.



Copyright: © 2021 by the authors. Licensee MDPI, Basel, Switzerland. This article is an open access article distributed under the terms and conditions of the Creative Commons Attribution (CC BY) license (<https://creativecommons.org/licenses/by/4.0/>).

1. Introduction

Among mineral nutrients, nitrogen (N) is the one required in the greatest amounts by plants, being an integral constituent of many organic compounds, such as nucleic acids, proteins, co-enzymes, chlorophyll, phytohormones and secondary metabolites [1]. In grapevine, N, after H, C and O, is usually the fourth most abundant element, representing 2–5% of plant biomass, and, in many cases, it is the most limiting factor for growth (i.e., vigor) and harvest yield [2]. Many studies conducted on grapevine highlighted the deep impact of N supply on plant reproductive capability as well as on grape berry metabolism and, finally, on berry composition [2–6]. In this view, the tight relationship between the rootstock/scion combination and N availability is emerging [7–9]. The N status of grapevine, like other perennial crops, depends on many factors, such as the acquisition of N from the soil, its distribution among annual organs and its reallocation from annual growth parts into both fruits and woody tissues [10–14]. In this context, the N content in grape berries, lost from the vineyard each year, has been estimated to be 2–3 kg of N per ton of fruit matter [2]. Nevertheless, a good management of N in vineyard must consider multifaceted aspects, in light of the fact that an excessive N supply can determine detrimental effects on the quality of grape berries and, therefore, of wine [4,5,8]. The achievement of this goal also comes via the improvement of the knowledge of the physiological, biochemical and molecular processes involved in the N metabolism of grapevine.

Although *Vitis* species could use different N forms, such as NO_3^- , NH_4^+ , urea and amino acids, NO_3^- , usually the predominant N form in vineyard soils, is the primary source of N for grapevine [2,15,16]. Consistent with the fluctuating availability of this anion in soil solution (from 100 μM to 10 mM and more), plants have evolved different root uptake systems with different affinity (high-affinity transport systems, HATSs, and low-affinity transport systems, LATs) and with both constitutive and inducible components [17–19]. The presence of HATSs rapidly responding to NO_3^- availability has been recently demonstrated in grapevine [20,21]. According to the proton gradient requirement for sustaining the $\approx 2\text{H}^+ : 1\text{NO}_3^-$ symporters, a concomitant induction of plasma membrane H^+ -ATPase in grapevine roots exposed to NO_3^- has also been described [20]. Interestingly, the capability to induce NO_3^- transporters in response to NO_3^- availability is strictly dependent on the scion/rootstock combination [21].

In grapevine, N assimilation can occur in both roots and leaves [2,22]. The process is performed by the well-characterized pathway that involves the reduction of NO_3^- to NH_4^+ through two steps catalyzed by nitrate reductase (NR) and nitrite reductase (NiR) and the subsequent assimilation catalyzed by glutamine synthetase (GS) and glutamate synthase (GOGAT), finally producing glutamic acid [1,22]. The contribution of the two organs depends on several factors, like N availability, C metabolism (i.e., availability of C skeletons), environmental conditions, tissue age and others [2,22–25]. Moreover, NO_3^- assimilation shows several connections with other biochemical pathways and responses, among which are amino acid metabolism, redox status and pH homeostasis [2,26,27]. Recently, Cochetel and co-workers published the first paper describing transcriptomic changes occurring in the roots of Riparia Gloire de Montpellier and 1103 Paulsen rootstocks in relation to NO_3^- availability [28]. Comparing these two genotypes, this study highlighted both specific responses and common changes in the gene expression patterns. Nitrogen-responsive genes involved in the uptake and assimilation of NO_3^- as well as genes encoding enzymes of the oxidative pentose phosphate (OPP) pathway were identified as being influenced by NO_3^- availability. According to the literature, the increase in OPP pathway activity is related to the typical metabolic adaptation of root tissues needed to satisfy the demand for reducing power [29,30]. In this context, the entity of the translocation of sugars from the photosynthetic tissues into roots affects the N assimilatory contribution of the two organs [2].

To our knowledge, to date, no proteomic investigation has studied the N responses in grapevine roots. Therefore, improvement of the information at translational and post-translational levels is desirable to better characterize the molecular and biochemical events evoked by changes in N availability in this perennial species. In the present work, we adopted biochemical and proteomic approaches to analyze, in the root of M4 grapevine rootstock, the responses occurring after the addition of NO_3^- to the nutrient solution in hydroponics. This rootstock genotype was selected on the basis of its good response to abiotic stress [31–35], which is contributing to the expansion of its use in viticulture. The biochemical evaluations were devoted to verifying the role played by roots in the response to NO_3^- resupply, monitoring key parameters. Moreover, since a holistic approach represents a good strategy to study the biological complexity [18,26,29], proteomic analysis was used to obtain a more comprehensive description of the first metabolic events involved in NO_3^- acquisition in roots of *Vitis*.

2. Results and Discussion

The activation of NO_3^- metabolism, which involves the modulation of specific transport systems and an assimilation pathway, is tightly linked to the external availability of the nutrient [20,21,29]. The rate at which plants induce these activities deeply affects their efficiency in using this mineral element in field conditions [36]. Moreover, studies performed on grapevine highlighted that, during the induction phase, the root organ plays an important role not only in N uptake from the soil, but also in N assimilation [2]. Starting from these considerations, the present work aimed at investigating in the roots of

M4 grapevine rootstock the responses to the addition of 10 mM NO_3^- in the hydroponic nutrient solution after a period of N starvation (see Materials and Methods for further details). First, key biochemical parameters were measured to define the timing of induction of the metabolic processes involved in the acquisition of NO_3^- . Afterwards, the changes in the root proteome were investigated.

2.1. Changes in Biochemical Parameters in Response to Nitrate

Biochemical analyses of key parameters in the roots of M4 were performed in order to define plant adaptations to renewed NO_3^- availability (Figure 1).

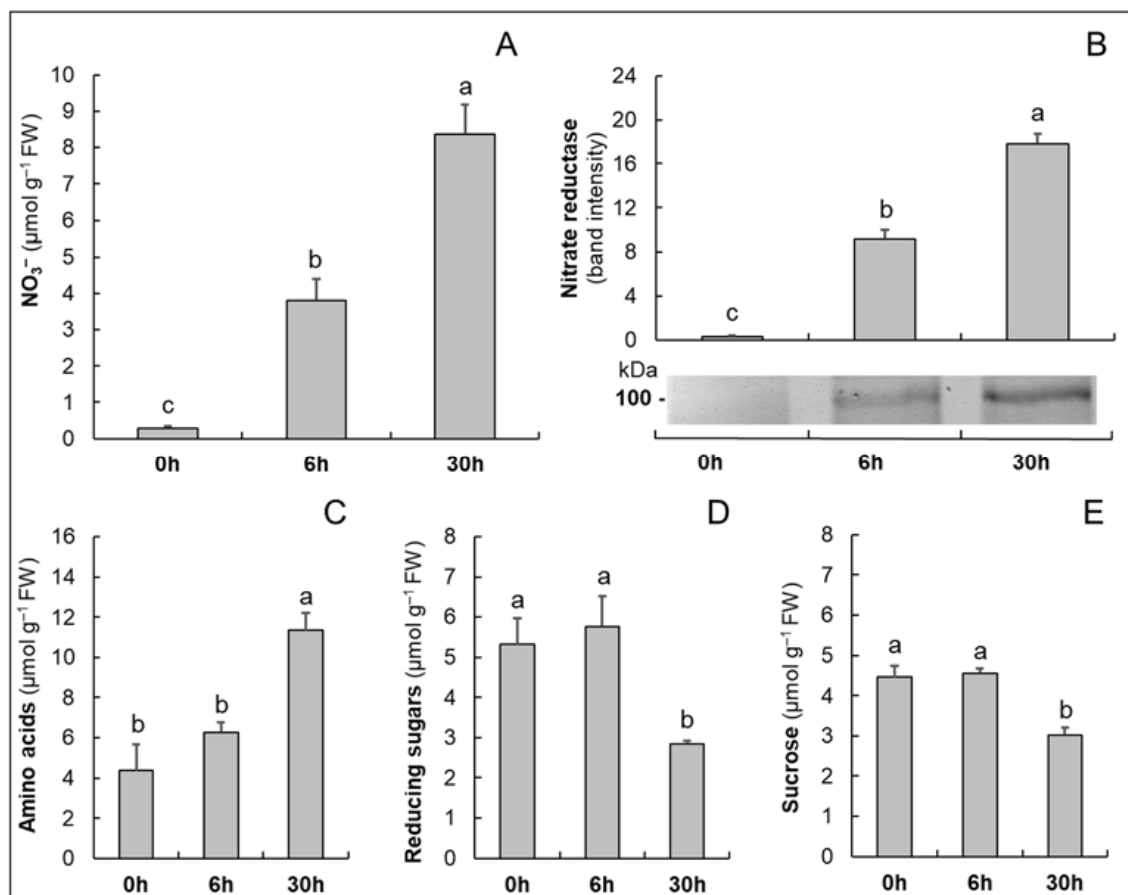


Figure 1. The time course of the changes in the contents of NO_3^- (A), in the accumulation of nitrate reductase evaluated by immunoblot analysis (B), and in the contents of amino acids (C), reducing sugars (D) and sucrose (E) in the roots of M4 grapevine rootstock, previously grown in the absence of N for 8 d (0 h) and incubated for a further 6 and 30 h in the presence of 10 mM NO_3^- . The values are means \pm SE ($n = 3$). Statistical significance was assessed by one-way ANOVA and the Holm–Šidák method. Different letters indicate significant differences ($p \leq 0.05$).

After the exposure of plants to NO_3^- , the contents of the anion in roots increased progressively within the first 30 h (Figure 1A), suggesting that NO_3^- uptake and accumulation were activated early and maintained throughout the treatment period (30 h). According to the role of NO_3^- as a signal for the induction of its assimilation [17], a parallel increase in NR abundance, evaluated by immunoblot analysis, occurred (Figure 1B). However, an increase in the content of amino acids was detected only after 30 h of treatment (Figure 1C), suggesting that a full activation of the NO_3^- assimilatory pathway was reached at this time point. In support of this conclusion, a decrease in reducing sugar and sucrose contents (Figure 1D,E) was measured only after 30 h of treatment, probably resulting from an increase in the use of C skeletons to sustain N assimilation.

This evaluation describes the typical metabolic changes involved in the acquisition and assimilation of NO_3^- well [18,36]. Moreover, these results allowed us to define, in M4 grapevine rootstock, the timing of these responses, which, interestingly, is highly consistent with those described for other grapevine genotypes [20,21,28]. Starting with this information, we performed the proteomic analysis, comparing the roots of N-starved plants (control plants, 0 h) with those of plants grown in the presence of 10 mM NO_3^- for 30 h.

2.2. Proteomic Analysis of M4 Root System

The proteomic analysis was performed by means of one-dimensional gel-liquid chromatography-mass spectrometry (GeLC-MS/MS), considering its suitability for the analysis of total proteomes in plant tissues [33,37]. Through this approach, it was possible to study the abundance of 461 proteins, with high reliability in identification and a good degree of comparability among samples and conditions (Table S1).

2.2.1. Functional Distribution of the Identified Proteins

The functional classification of the identified proteins, reported in detail in Table S2, was conducted according to the MapMan4 ontology [38]. The identified proteins fell into 15 functional categories (Figure 2). Many of them belonged to four categories, “Protein” (24%), “Not assigned-annotated” (18%), “Carbon and energy metabolism” (13%) and “Enzymes/Coenzyme metabolism” (8%). Regarding the proteins that fell into the “Not assigned-annotated” category, in order to better define their functional role, a supplemental investigation was performed, using the UniProt database (<https://www.uniprot.org/>, accessed on 1 December 2020) and the basic local alignment search tool (BLAST). However, no information, or very fragmentary information, was available for proteins classified in the “Not assigned-not annotated” group, which corresponded to 5% of total identified proteins.

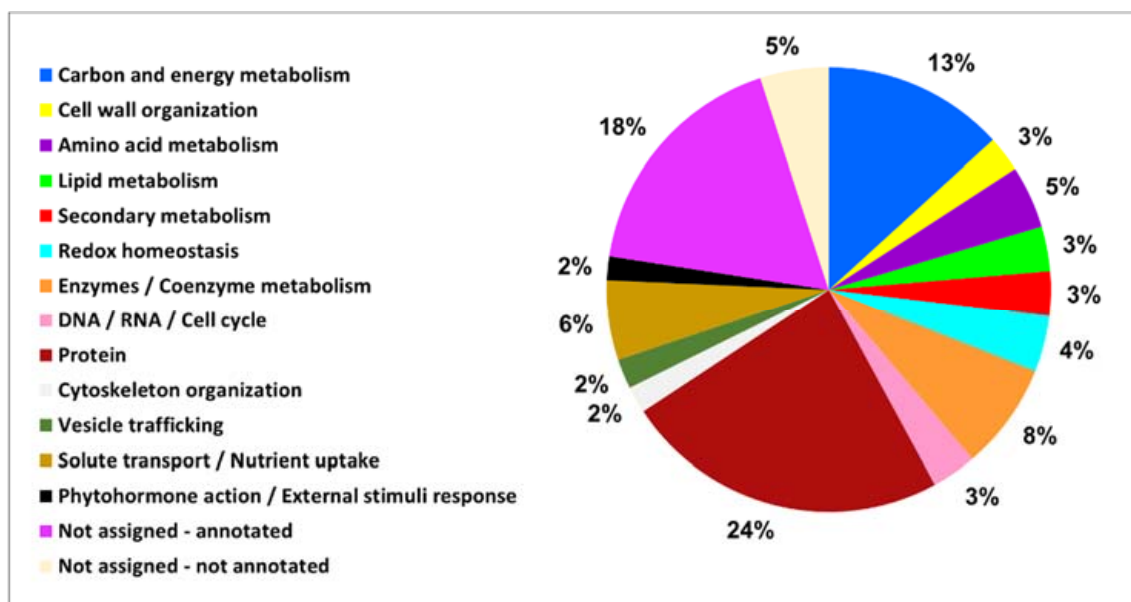


Figure 2. Functional distribution of all the identified proteins in the roots of M4 grapevine rootstock. Proteins were grouped in categories according to BIN ontology.

Statistical analysis highlighted 119 proteins that significantly changed in abundance after the exposure of the plants to 10 mM NO_3^- for 30 h. Figure 3 shows their functional distribution. Among these proteins, 68 increased or appeared while 51 decreased or disappeared. Almost a half (46%) of the proteins that increased in abundance belong to the

“Protein” category. Interestingly, some other functional categories included proteins that were accumulated in a higher abundance in response to NO_3^- supply, such as “Carbon and energy metabolism”, “Not assigned-annotated”, “Enzyme/Coenzyme metabolism” and “Amino acid metabolism” (13%, 10%, 9% and 6%, respectively). However, many of the proteins that decreased or disappeared were classified into the categories “Not assigned-annotated”, “Protein”, “Enzyme/Coenzyme metabolism” and “Carbon and energy metabolism” (31%, 16%, 10% and 8%, respectively).

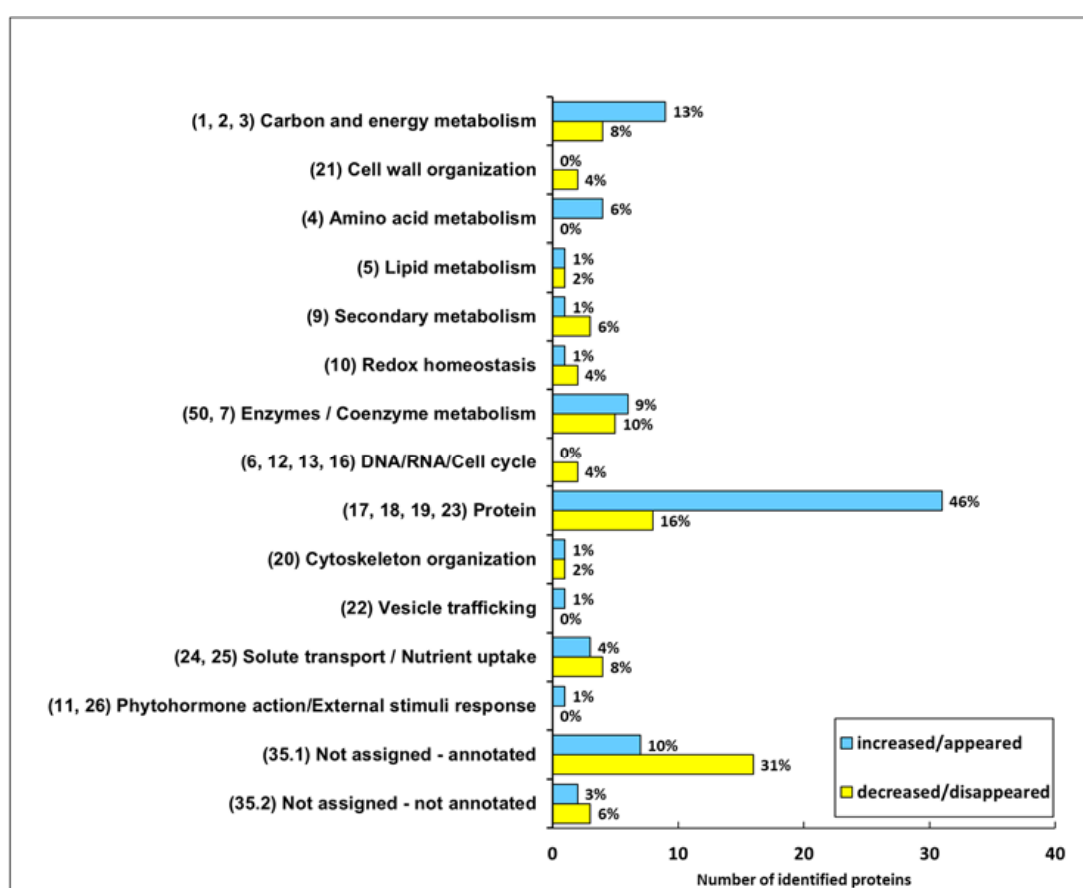


Figure 3. Functional distribution of the differentially accumulated proteins in roots of M4 grapevine rootstock after exposure of the plants to 10 mM NO_3^- . Proteins were grouped in categories according to BIN ontology (codes reported in brackets). The percentage refers to the total number of proteins having the same trend: blue bars, proteins that increased/appeared; yellow bars, proteins that decreased/disappeared.

Overall, the functional distribution of the NO_3^- -responsive proteins is consistent with the typical adaptations described in plants, and specifically in root tissues, in response to the availability of this nutrient [26,39,40]. Among them, modifications are evident in pathways related to the production of energy and C skeletons as well as broad changes in protein metabolism. In addition, several other metabolic traits were affected by the nutritional treatment. In details, Table 1 includes all the proteins that changed in abundance in response to NO_3^- .

Table 1. Proteins differentially accumulated in response to 10 mM NO₃[−] for 30 h in roots of M4. Proteins are grouped according to functional classification (Figure 3). Subtitles report functional categories and their bin codes. #: identification number (group). **UIP**: number of unique identified peptides. **Score**: MS/MS search score. **Δ(nit/con)**: fold changes expressed as the ratio between the protein abundance in NO₃[−]-treated plants (nit, 30 h) and in the control N-starved plants (con, 0 h). **Blue cells**: proteins that increased in abundance. **Yellow cells**: proteins that decreased in abundance. **s**: statistical significance assessed by Student's *t*-test (*n* = 3) (* *p* < 0.05, ** *p* < 0.01). ^a: protein annotated by BLAST. In *italics*: additional information from UniProt. **New**: not detected in control plants; **d.**: disappeared, not detected in NO₃[−]-treated plants.

#	Accession Number	UIP	Score	Protein Name	Δ (nit/con)	s
Carbon and energy metabolism (1, 2, 3)						
28	A5B118	12	167.9	Fructose-bisphosphate aldolase	2.01	*
23	A5CAF6	12	191.3	Phosphoglycerate kinase	1.83	*
122	F6I1P0	6	80.5	Pyruvate dehydrogenase E1 component subunit beta	0.22	**
251	A5AY34	4	45.9	Oxidored_q6 domain-containing protein	4.34	*
2	A5AYU8	18	330.6	ATP synthase subunit beta	0.63	**
150	D7T300	6	54.9	ATP synthase subunit O, mitochondrial I ^a	new	*
14	F6HGZ9	14	160.9	Sucrose synthase	new	*
257	Q1PSI9	4	43.7	L-idonate 5-dehydrogenase	15.59	**
323	A0A438D9B1	3	36.8	Glucose-6-phosphate 1-dehydrogenase	new	**
169	A0A438HWY8	5	66.2	Probable 6-phosphogluconolactonase	0.29	*
64	F6HGH4	8	120.0	6-phosphogluconate dehydrogenase, decarboxylating	9.40	**
239	D7TJI9	4	50.4	Pyruvate decarboxylase	0.34	**
77	F6HUI7	8	88.3	RmlD_sub_bind domain-containing protein	3.34	*
Cell wall (21)						
131	A0A438KK24	6	75.1	Caffeoyl-CoA O-methyltransferase	0.36	**
54	F6GSZ7	9	119.1	Omega-hydroxypalmitate O-feruloyl transferase ^a	0.63	*
Amino acid metabolism (4)						
3	F6HMN8	18	266.7	5-methyltetrahydropteroyltriglutamate-homocysteine S-methyltransferase	2.90	*
73	A0A438GBL8	8	106.4	Acetohydroxy-acid reductoisomerase	6.64	*
30	F6I5Y5	12	159.3	D-3-phosphoglycerate dehydrogenase	1.66	*
140	F6H0X2	6	67.6	Phospho-2-dehydro-3-deoxyheptonate aldolase	2.39	**
Lipid metabolism (5)						
51	F6I1D6	9	142.9	Non-specific phospholipase C3 ^a	0.52	**
462	A0A438FDG5	2	20.2	Enoyl-CoA delta isomerase 3	1.63	*
Secondary metabolism (9)						
173	F6HHQ7	5	65.2	Putative acetyl-CoA acetyltransferase, cytosolic 2 ^a	0.39	*
314	A0A024FS61	3	39.3	Polyphenol oxidase	4.73	*
415	A0A438ESC9	2	25.1	3-isopropylmalate dehydratase small subunit 3	0.09	*
86	F6I076	7	107.7	CN hydrolase domain-containing protein	0.05	**

Table 1. Cont.

#	Accession Number	UIP	Score	Protein Name	Δ (nit/con)	s
Redox homeostasis (10)						
185	G1JT87	5	59.7	Glutaredoxin-dependent peroxiredoxin	0.41	*
269	D7T6T0	4	39.8	Glutaredoxin-dependent peroxiredoxin	4.16	*
330	A9UFY2	3	36.1	Thioredoxin h-type	0.45	*
Enzymes/Coenzyme metabolism (50, 7)						
136	D7TKJ3	6	71.1	Ferredoxin-NADP reductase, chloroplastic	new	**
148	D7SNB1	6	58.9	Salutaridine reductase ^a	0.41	*
11	K9N4H5	14	213.1	Mitochondrial aldehyde dehydrogenase 2B8	0.65	*
119	A5BHH9	6	80.8	NADH-cytochrome b5 reductase	0.29	*
41	F6H5H5	10	156.0	Trans-resveratrol di-O-methyltransferase ^a	1.63	**
458	A0A438CVH9	2	20.5	UDP-glycosyltransferase 74F2	7.77	*
105	A0A438KGT6	6	98.7	Glucan endo-1,3-beta-D-glucosidase	0.27	**
151	A0A438ITG1	5	93.1	Putative cysteine protease RD21B	0.36	**
81	A0A438EKJ2	7	116.9	Phosphopyruvate hydratase (synonym: Enolase)	2.28	**
154	A0A438D2Y0	5	83.1	Phosphoglycerate mutase	2.00	**
38	F6GTM7	11	160.1	Adenosylhomocysteinase	4.96	*
DNA/RNA/Cell cycle (6, 12, 13, 16)						
280	A5B6U5	4	34.5	Proliferating cell nuclear antigen	0.05	*
378	F6GSZ1	2	31.5	RRM domain-containing protein	0.61	*
Protein (17,18,19,23)						
300	A5AXI6	3	43.0	60S acidic ribosomal protein P0	24.11	**
126	A5BUU4	6	78.2	40S ribosomal protein SA	4.43	**
217	A5C4J2	4	58.0	40S ribosomal protein S19-3 ^a	2.38	*
443	A5AJ83	2	22.4	Ribosomal_S10 domain-containing protein	4.27	*
135	A0A438KA42	6	72.8	Guanine nucleotide-binding protein subunit beta-like protein	3.44	**
375	F6HLE8	2	33.4	Ribosomal_S7 domain-containing protein	3.47	*
171	A0A438C2W6	5	65.7	Aspartate-tRNA ligase	2.44	*
37	F6HXZ5	11	164.6	Eukaryotic initiation factor 4A-2 ^a	2.50	**
407	F6GTY8	2	26.2	Tr-type G domain-containing protein	10.31	**
149	A0A438CSH7	6	57.0	Elongation factor 1-gamma	new	*
128	F6H4T7	6	77.2	Tr-type G domain-containing protein	20.06	**
346	A0A438JTD3	3	33.5	Dolichyl-diphosphooligosaccharide-protein glycosyltransferase 48 kDa subunit	new	*
44	D7TBD9	10	143.7	Alpha-MPP	0.39	*
99	A5ANH8	7	82.5	Probable mitochondrial-processing peptidase subunit beta, mitochondrial ^a	3.78	*
176	A0A438DUK9	5	63.2	Protein disulfide-isomerase	13.28	**
335	A0A438K994	3	35.3	Citrulline-aspartate ligase	7.32	**
47	D7SIX7	10	128.0	Serine/threonine-protein phosphatase 2A 65 kDa regulatory subunit A beta isoform ^a	0.56	*
108	A0A438G7L8	6	97.4	Glutathione S-transferase U10	2.49	*
337	F6I510	3	34.9	Putative glutathione S-transferase parC ^a	2.94	*

Table 1. Cont.

#	Accession Number	UIP	Score	Protein Name	Δ (nit/con)	s
Protein (17,18,19,23)						
448	F6GT86	2	21.5	Glutathione S-transferase ^a	4.05	*
232	A0A438KHW4	4	53.1	Glutathione transferase	1.65	*
452	F6HYG1	2	21.4	Heat shock 70 kDa protein 15-like ^a	new	*
1	F6HNX5	20	361.7	Putative heat shock cognate protein 2 ^a	2.04	**
370	A0A438K358	2	38.1	Hsp70-Hsp90 organizing protein 1	new	**
317	A0A438D490	3	38.2	Heat shock cognate protein 80	new	*
107	D7SLM9	6	98.0	RuBisCO large subunit-binding protein subunit beta, chloroplastic ^a	5.54	**
145	F6GUM1	6	65.0	E1 ubiquitin-activating enzyme	6.77	**
379	A0A438J7X4	2	31.5	Ubiquitin-conjugating enzyme E2-17 kDa	1.48	*
147	A0A438KGZ1	6	62.4	Proteasome subunit beta	0.52	*
420	D7SKV3	2	24.4	Proteasome subunit beta	6.25	*
388	A0A438EWK5	2	29.3	26S proteasome regulatory subunit 7	8.65	*
322	F6HT17	3	36.9	PCI domain-containing protein	3.30	*
93	A0A438JN39	7	93.2	Serine carboxypeptidase-like 7	0.48	*
115	D7T3Q1	6	85.9	Glucose acyltransferase 1 ^a	0.48	**
195	A5C1I0	5	57.1	Carboxypeptidase	0.71	*
26	F6H7H1	12	172.6	Aspartic proteinase A1 ^a	0.56	*
396	A0A438K8Z1	2	28.0	Aminopeptidase	new	**
400	A0A438EKP3	2	27.0	Ankyrin repeat domain-containing protein 2A	0.21	*
228	A0A438JPS3	4	53.8	GTP-binding nuclear protein Ran1B	12.55	**
Cytoskeleton organization (20)						
4	A5ATG8	17	307.8	Tubulin beta chain	0.78	*
347	A0A438F6R2	3	33.3	T-complex protein 1 subunit gamma	4.31	**
Vesicle trafficking (22)						
144	D7T9L8	6	65.0	Coatomer subunit delta	6.58	**
Solute transport/Nutrient uptake (24, 25)						
306	F6I0Z8	3	40.4	Plasma membrane 22 aquaporin	2.81	**
203	Q9FS46	4	70.6	Putative aquaporin	0.65	**
216	A5AQ65	4	58.1	Mitochondrial outer membrane protein porin 2 ^a	0.38	**
325	A0A438CTH2	3	36.5	Mitochondrial outer membrane protein porin of 34 kDa	0.43	**
246	A0A438FMR0	4	46.7	Ferredoxin–nitrite reductase, chloroplastic	new	**
29	A5AP38	12	162.2	Glutamine synthetase (cytosolic ^a)	0.65	*
321	A0A438E3X6	3	37.1	Ferritin	10.77	**
Phytohormone action/External stimuli response (11, 26)						
224	F6H6V6	4	54.5	Senescence-associated carboxylesterase 101 ^a	4.18	**
Not assigned-annotated (35.1)						
46	A0A438KRJ6	10	138.5	Annexin (D2 ^a)	1.44	**
403	A0A438JYU9	2	26.9	Dipeptide epimerase	8.06	**
76	D7SJF5	8	95.2	Cystathionine beta-synthase family protein ^a	5.70	**
158	A5BM68	5	73.7	TCTP domain-containing protein	1.81	*
48	A0A438J6W5	10	124.3	Glutelin type-A 2	0.11	**
230	A0A438KKU7	4	53.6	Stem-specific protein TSJT1	0.26	**

Table 1. Cont.

#	Accession Number	UIP	Score	Protein Name	Δ (nit/con)	s
Not assigned-annotated (35.1)						
89	A0A438JUI6	7	104.2	MLP-like protein 34	1.49	**
165	A0A438JUL6	5	68.5	MLP-like protein 43	3.25	*
42	F6GTA6	10	147.7	PHB domain-containing protein	0.54	**
91	D7TNE5	7	97.3	PHB domain-containing protein	0.51	*
106	A0A438J2L0	6	98.2	Chalcone-flavonone isomerase family protein (synonym: <i>Chalcone isomerase</i>)	0.61	*
110	A0A438BSC8	6	92.9	NAD(P)H dehydrogenase (quinone)	0.40	*
215	D7T2N7	4	59.9	Late embryogenesis abundant protein	0.58	*
265	D7T3J3	4	41.3	Lea14-A, putative ^a	0.26	**
289	F6H6H8	3	48.8	Proline iminopeptidase	d.	*
387	A5BM29	2	29.4	Glyco_hydro_18 domain-containing protein	0.11	**
104	D7T7N4	6	102.7	NTF2 domain-containing protein	0.28	*
112	A0A438GQU3	6	91.0	RRM domain-containing protein	0.02	**
199	A0A438IQU7	5	47.6	Kunitz trypsin inhibitor 2	d.	*
180	A0A438C6P2	5	62.0	Major allergen Pru ar 1	0.14	*
395	A5AJB3	2	28.1	Plastid-lipid-associated protein, chloroplastic	d.	*
208	A0A438JVD2	4	64.1	Chitin-binding type-1 domain-containing protein	0.42	**
345	F6HIK4	3	33.9	Peroxidase	4.52	*
Not assigned-not annotated (35.2)						
72	A5C8L8	8	106.9	Pyr_redox_2 domain-containing protein	5.10	**
95	D7TA35	7	88.6	Usp domain-containing protein	4.39	*
273	D7U4I8	4	38.5	Usp domain-containing protein	d.	**
142	A0A438JK35	6	66.9	Bifunctional epoxide hydrolase 2	0.01	*
167	A5AEX6	5	67.0	DLH domain-containing protein	0.75	*

2.2.2. Proteomic Changes Involved in Nitrogen Acquisition and in Carbon and Energy Metabolism

The proteomic analysis revealed the appearance of ferredoxin-nitrite reductase (#246) in the roots of plants exposed to NO_3^- . According to the increases in NR abundance and in amino acid levels (Figure 1B,D), this result confirms the activation of the primary N assimilation pathway. Moreover, the appearance of ferredoxin-NADP reductase (#136) and glucose-6-phosphate 1-dehydrogenase (#323), as well as the dramatic increase in 6-phosphogluconate dehydrogenase (#64), is in agreement with a higher metabolic demand for NADPH, that in non-photosynthetic tissues is fulfilled by the OPP pathway [26,29]. However, cytosolic glutamine synthetase (#29) decreased in abundance in response to NO_3^- , suggesting a reduction in N recycling. This behavior probably mirrors the effect of NO_3^- availability on the plant N status, and the consequent change in protein and amino acid catabolism [41].

At the same time, several glycolytic enzymes, such as fructose-bisphosphate aldolase (#28), phosphoglycerate kinase (#23), phosphoglycerate mutase (PGM, #154) and enolase (#81), increased in abundance in response to NO_3^- , according to a higher demand for C skeletons needed for N assimilation [42]. Among them, the peculiar role played by PGM that, even if it catalyzes a non-rate-limiting step in glycolysis, is involved in the recycling of glyceraldehyde-3P produced by the OPP is highlighted [26,29].

Interestingly, the concomitant decrease in the E1 component of pyruvate dehydrogenase (#122) suggests that an activation of anaplerotic reaction(s) occurred, rather than an upsurge of carbon oxidation through the Krebs cycle. In this view, it could be observed that the levels of the β subunit of ATP synthase (#2), mitochondrial aldehyde dehydrogenase

(#11), NADH-cytochrome b5 reductase (#119) and NAD(P)H dehydrogenase (#110) also decreased after the addition of NO_3^- . Once again, this behavior could be ascribed to a shift in the balance between N recycling and assimilation.

In support of the above results, the activation of C metabolism in roots was accompanied by a decrease in the content of reducing sugars and sucrose (Figure 1D,E). In this view, it is interesting to observe that only in roots of plants exposed to NO_3^- was a sucrose synthase (#14) detectable, an enzyme that plays a pivotal role in determining the sink strength necessary to import photoassimilates from the source organs [43]. This result suggests that the sink strength of the root system increases during the early phases of exposure to NO_3^- . Hence, it is possible that this response could have a role in the scion/rootstock relations and in the N use efficiency of different grafting combinations.

2.2.3. Proteomic Changes Involved in Protein and Amino Acid Metabolism

The present study found that many proteins involved in protein synthesis, modification and degradation changed in abundance in response to NO_3^- availability (Table 1). These include ribosomal proteins (#300, #126, #217, #443, #375) as well as initiation (#37) and elongation factors (#407, #149, #128). These changes agree with recent literature that highlights a resumption of these metabolic activities among the responses of N-starved plants to renewed availability of NO_3^- , in *Arabidopsis* (*Arabidopsis thaliana* L.) and maize (*Zea mays* L.) [26,39,40]. According to an activation of protein synthesis, a few heat shock proteins (#452, #1, #370, #317, #107), known to be involved in protein folding [44], were also more abundant in NO_3^- -treated plants. At the same time, the proteomic analysis revealed a different accumulation of proteins operating in the proteasome (#147, #420, #388) and in ubiquitination (#145, #379), suggesting an increase in protein turnover.

Conversely, several proteases, such as two carboxypeptidases (#93, #195), a putative cysteine protease RD21B (#151) and an aspartic proteinase A1 (#26), decreased in abundance after the reintroduction of NO_3^- . Considering that some of these proteins have extracellular localization, these results support the hypothesis that during N starvation, roots are able to intensify the exudation of proteases, probably in order to mobilize N from peptides and proteins in the rhizosphere [45]. Interestingly, the secretion of such enzymes has also been observed in the absence of microorganisms [45], and, therefore, it is possible that it occurs in plants grown in hydroponic systems.

The metabolism of a few amino acids seemed to be positively affected upon NO_3^- resupply. The proteomic analysis revealed an increase in the abundance of enzymes involved in the biosynthesis of methionine (#3, 5-methyltetrahydropteroyltriglutamate-homocysteine S-methyltransferase; #38, adenosylhomocysteinase), isoleucine (#73, acetohydroxy-acid reductoisomerase) and serine (#30, D-3-phosphoglycerate dehydrogenase). Moreover, an increase in the level of phospho-2-dehydro-3-deoxyheptonate aldolase (#140) was detected, being the first enzyme of the shikimate pathway, which is involved in the synthesis of aromatic amino acids. This result is in agreement with studies on other plant species that describe an activation of the synthesis of amino acids in order to sustain the reactivation of protein synthesis [26,40,46].

2.2.4. Other Biochemical Functions Affected by Nitrate Resupply

A few enzymes involved in cell wall lignification, such as a caffeoyl-CoA O-methyltransferase (CCOMT, #131) and an omega-hydroxy-palmitate O-feruloyl transferase (OHFT, #54), decreased in abundance in response to NO_3^- availability. It is interesting to observe that the late embryogenesis abundant protein Lea14-A (#215), described as able to positively regulate the deposition of lignin under stress conditions [47], followed a similar trend, as well as a glucan endo-1,3-beta-D-glucosidase (#105). These results are consistent with the well-documented reprogramming of the root development process that occurs in response to NO_3^- [39,48,49]. Moreover, the different behaviors of two peroxidases (POXs, #208, #345) are noteworthy, which showed an opposite response to NO_3^- . Although a role of POX in the lignification process was proposed, the trends of CCOMT and OHFT strongly weaken

this hypothesis and suggest a context in which this process seems reduced. However, considering the very multifaceted role of these enzymes, it is interesting to highlight that an increase in peroxidase and polyphenol oxidase (PPO) activities was described in grapevine during the adventitious rooting process [50]. Our proteomic analysis identified a PPO (#314) positively affected by NO_3^- exposure, highlighting a possible analogy.

Other proteins involved in phenolic metabolism changed in abundance in response to NO_3^- . Among them, a decrease in chalcone isomerase (#106), an enzyme that catalyzes the isomerization of naringenin chalcone to naringenin flavanone in the flavonoid pathway, was observed. This result agrees with the well-known reduction in phenylpropanoid metabolism occurring after NO_3^- resupply to N-starved plants [26,51–54]. At the same time, we observed an increase in trans-resveratrol di-O-methyltransferase (#41), which suggests different effects on specific traits of the phenylpropanoid metabolism. This enzyme catalyzes the formation of pterostilbene from resveratrol, a compound with antimicrobial and antifungal properties [55,56]. The specific role of this molecule in roots remains to be clarified, however, it was proposed that its increase upon high N availability could participate in promoting root relations with the rhizosphere community. Although further studies are needed, attention could be focused on the interplay occurring between plants and other organisms in the soil. In this view, it is interesting to note that our proteomic analysis identified a proline iminopeptidase (#265) that decreased in abundance in response to NO_3^- . Considering that this peptidase is induced by bacteria and seems to participate in virulence [57], our results suggest that NO_3^- availability could reduce root susceptibility to pathogens.

Moreover, our proteomic analysis revealed changes of a few typical stress-responsive proteins. Some of them, such as major allergen Pru ar 1 (#199), chitin-binding type-1 (#395) and PHB (#42, #91), decreased, whilst others, such as MLP-like protein 34 and 43 (#89, #165) and annexin D2 (#46), increased in response to NO_3^- . Given the paucity of the current information for many of them [58], it is difficult to fully understand the biological meaning of these results. Recently, Wang and co-workers [59] provided new information about MLP-like protein 43, highlighting its participation in the drought responses mediated by ABA. In detail, these authors described the involvement of this protein in the response to oxidative stress as well as in the modulation of primary metabolism. Further analyses may help to clarify possible roles of this protein in the metabolic changes induced by NO_3^- . Although, for annexin, an interesting role in the differentiation/growth processes at the membrane level is emerging [60], and in view of the morphological responses evoked by NO_3^- in root system, further work is necessary to define its specific role in grapevine rootstock.

The available literature describes changes in the expression of genes involved in redox metabolism upon NO_3^- provision in Arabidopsis [26,39]. Our study revealed that NO_3^- positively affected a glutaredoxin-dependent peroxiredoxin (#269) and cystathionine beta-synthase family protein a (#76), whilst another glutaredoxin-dependent peroxiredoxin (#185) and a thioredoxin h-type (#330) decreased. Considering their involvement in the regulation of the oxidative state of sulfhydryl groups and in the S-glutathionylation of proteins [61,62], this result underlines the crucial role of the redox system in the modulation of the metabolic adjustment evoked by increased NO_3^- availability. Reinforcing this hypothesis, we also found four glutathione transferases (#108, #337, #448, #232) that showed an upsurge in abundance in response to NO_3^- supply. Interestingly, future redox proteomics studies could be very useful to better clarify the role of redox-related post-translational modifications in response to N supply in plants.

Overall, our results highlight the important role of roots in the plant adaptations to changes in N availability. As previously described in other plant species, this study confirms that grapevine roots show a typical metabolic activation involved in the acquisition of this macronutrient. Moreover, this investigation brings evidence of interesting relationships between N availability and root–rhizosphere dialog. This new knowledge paves the way for further studies aimed at characterizing key factors involved in N use efficiency in this pluriannual species. Other interesting aspects that deserve attention in the future are the plant responses in field conditions, the adaptability to N availability in different graft combinations and the final outcomes in grape quality.

3. Materials and Methods

3.1. Plant Material and Nutritional Treatments

The M4 [(*V. vinifera* × *V. berlandieri*) × *V. berlandieri* cv. Resseguier no. 1] grapevine rootstock genotype was obtained from Vitro Hellas (Niseli Alexandra, Greece, <https://www.vitrohellas.gr/en/home>, accessed on 1 August 2020). A scheme of the experimental design is shown in Figure 4. Plants, previously grown in peat soil, were flared, gently washed to remove residual particles of soil from the roots and then transferred to a hydroponic system. The experiments were conducted in a growth chamber with a 16/8 h day/night regime, at 26/22 °C, constant relative humidity of 65% and PPFD of 300 $\mu\text{mol m}^{-2} \text{s}^{-1}$. All hydroponic solutions were continuously aerated by an electric pump. To allow adaptation to hydroponic conditions, plants were grown for 5 weeks in a nutrient solution (0.77 mM K_2SO_4 , 0.65 mM MgSO_4 , 0.51 mM KH_2PO_4 , 0.4 mM CaSO_4 , 100 μM Fe-EDTA, 50 μM KCl, 10 μM H_3BO_3 , 1 μM MnSO_4 , 0.5 μM CuSO_4 , 0.5 μM ZnSO_4 , 0.35 μM Na_2MoO_4 , pH = 6.1) containing 0.25 mM $\text{Ca}(\text{NO}_3)_2$ (i.e., low N input). The solution was replaced weekly. After this period, the plants were transferred into new nutrient solutions without N. After 8 days of N starvation (control plants, 0 h), plants were transferred to a fresh growing solution containing 10 mM KNO_3 . The start of the experiments coincided with the start of the light period. The plants were sampled at 0 h and after 6 and 30 h of treatment. Roots were rinsed with water, blotted with paper towels, and then immediately frozen in liquid N_2 . Each biological sample was composed of roots collected from three plants. Samples were stored at -80°C .

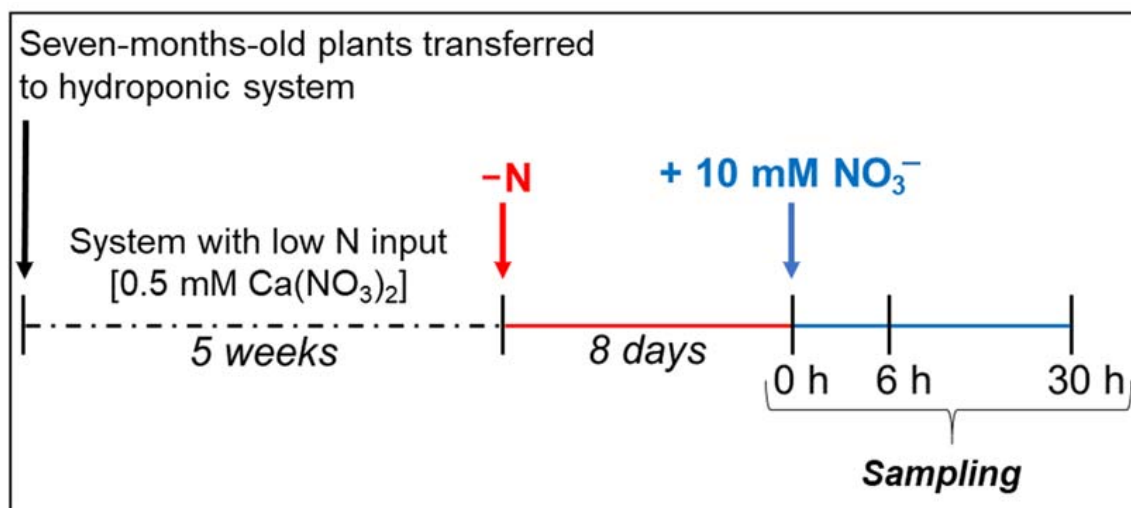


Figure 4. Growth experiment design and nutritional treatments. Further details are reported in the Material and Methods.

3.2. Determination of the Contents of Nitrate, Amino Acids, Sucrose and Reducing Sugars

Nitrate was extracted from the tissues by homogenizing the samples in 4 volumes of distilled water and heating at 50 °C for 15 min. The homogenate was centrifuged at

12,000× *g* for 20 min to obtain a clarified supernatant. An aliquot of the supernatant was used for the determination of NO₃[−] concentration, according to Cataldo et al. [63].

Amino acids and total sugars were extracted in perchloric acid (PCA) as previously described by Meggio and co-workers [31]. The contents of total amino acids were measured by the ninhydrin method [64]. The contents of total soluble sugars were determined by boiling an aliquot of the PCA extract for 1 h before neutralization. Sugar concentrations were then measured according to the colorimetric method of Nelson [65]. All the analyses were replicated on three independent biological samples (*n* = 3) and compared by the ANOVA test (*p* < 0.05, Holm–Šidák method).

3.3. Protein Extraction

Protein extraction was performed as previously described [33]. Briefly, frozen powdered samples (1 g) of three biological samples for each experimental condition (*n* = 3) were finely powdered in liquid N₂ using a pestle and mortar, adding 5% (*w/w*) of polyvinylpyrrolidone. The total protein fraction was extracted by adding 5 volumes of phenol and an adequate volume of aqueous buffer [0.7 M sucrose, 10 mM Na₂-EDTA, 4 mM ascorbic acid, 0.2% (*v/v*) Triton X-100, 1 mM PMSF, 0.1 mg mL^{−1} Pefabloc and 0.4% (*v/v*) β-mercaptoethanol]. The protein fraction was then purified by methanol-based and acetone precipitation [66]. The final pellet was then dissolved in SDS buffer [150 mM Tris-HCl pH 6.8, 10% (*w/w*) glycerol, 2% (*w/w*) sodium dodecyl sulfate (SDS), 2% (*v/v*) β-mercaptoethanol] and incubated at 95 °C for 5 min. The sample was centrifuged at 10,000× *g* for 10 min and the supernatant stored at −80 °C until further use. The protein concentration was determined by the 2-D Quant Kit (GE Healthcare Europe GmbH, Freiburg, Germany).

3.4. Immunoblot Analyses

Protein samples (10 µg) were diluted with a volume of SDS buffer with 0.01% (*w/v*) bromophenol blue, heated for 5 min at 95 °C and then separated by SDS-polyacrylamide gel electrophoresis (SDS-PAGE) using 10% (*w/v*) polyacrylamide gel [67]. The samples were then electrophoretically transferred onto a polyvinylidene difluoride (PVDF) filter using a semidry blotting system (NovaBlot, Pharmacia, Sweden) with a buffer containing 10 mM 3-cyclohexylamino-1-propanesulphonic acid (CAPS, pH 11 with NaOH) and 10% (*v/v*) methanol. Filters were blocked for 1 h with TBS-T buffer [50 mM Tris-HCl (pH 7.6), 200 mM NaCl, and 0.1% (*v/v*) Tween 20] supplemented with 3% (*w/v*) albumin. The TBS-T buffer was used as an incubation medium throughout the procedure. Filters were incubated overnight at 4 °C with primary polyclonal antibodies against nitrate reductase using a 1:1,250 dilution (Agrisera, Vännäs, Sweden, AS08 310). After washing with TBS-T, the filters were incubated for 2 h at room temperature with a secondary antibody (alkaline phosphatase-conjugated anti-rabbit immunoglobulin G). The blot was developed with nitroblue tetrazolium and 5-bromo-4-chloro-3-indolyl phosphate (FAST BCIP/NBT, Sigma). The analysis was performed on three biological samples (*n* = 3), and the quantification of the signals was conducted through densitometric analysis by using the software ImageJ (<https://imagej.net/>, accessed on 1 August 2020).

3.5. Gel Electrophoresis and In-gel Digestion

Gel electrophoresis, in-gel digestion and mass spectrometry analyses were performed as previously described [40], with the following refinements. Briefly, 30 µg of proteins were separated on an SDS-PAGE on 16% (*w/v*) polyacrylamide gel [67], until samples ran a 3 cm length. After Coomassie brilliant blue staining, the blank portions of the gels as well as the regions above 250 kDa or below 12 kDa were removed. Each line was cut into 3 regular slices (10 × 10 × 0.75 mm). Each slice was then treated as an independent sample. In-gel digestion was performed according to Prinsi and co-workers [40]. The extracted peptides were finally dissolved in 0.1% (*v/v*) formic acid (FA).

3.6. Mass Spectrometry Analysis

All mass spectrometry experiments were conducted with an Agilent 6520 Q-TOF mass spectrometer equipped with an HPLC Chip Cube (Agilent Technologies, Cernusco sul Naviglio, Italy), as previously described [33], with some refinements. In detail, the peptides were eluted by applying a 100 min non-linear gradient of acetonitrile from 5% to 50% (*v/v*) in acidic conditions (FA 0.1% *v/v*) at 0.4 $\mu\text{L min}^{-1}$. The mass spectrometer was run in positive ion mode and MS scans were acquired over a range from 300 to 3000 mass-to-charge ratio (*m/z*) at 4 spectra s^{-1} . MS/MS scans were acquired over a range from 50 to 3000 mass-to-charge ratio (*m/z*) at 3 spectra s^{-1} . Precursor ions were selected by auto-MS/MS with a maximum of 4 precursors per cycle and active exclusion set at 2 spectra for 0.1 min. Sample profiles were reconstructed by combining the chromatograms obtained for all three slices into which they were divided. Analysis of MS/MS spectra was performed by Spectrum Mill MS Proteomics Workbench (Rev B.04.00.127, Agilent Technologies). Carbamidomethylation of cysteine was set as a fixed modification while the oxidation of methionine was a variable modification. Trypsin was selected as the enzyme for digestion, accepting 2 missed cleavages per peptide. For spectrum interpretation, the search was conducted against the *Vitis* (ID 3603) protein database (December 2020, 167,581 entries) downloaded from UniProtKB/Swiss-Prot (<http://www.uniprot.org/>, accessed on 1 February 2021) and concatenated with the reverse one. The mass spectrometry proteomics data have been deposited in the ProteomeXchange Consortium [68] via the PRIDE partner repository with the data set identifier PXD025212. The threshold used for protein identification was peptide false discovery rate (FDR) $\leq 1\%$ and number of unique peptides per protein ≥ 2 . Peptide quantification was obtained as the spectrum intensity (SI) of the precursor. Protein quantification was obtained by summing the SIs of all the identified peptides in the protein. Protein abundance was normalized as the percentage with respect to the abundance of all validated proteins in the sample (%(SI)), summing all validated peptides in the 3 slices [33]. The analysis was performed using three biological samples for each condition ($n = 3$). Statistical significance was assessed by a Student's *t*-test ($p < 0.05$). The identified proteins were classified into metabolic functional categories according to the MapMan4 BIN ontology [38].

Supplementary Materials: The following are available online at <https://www.mdpi.com/article/10.3390/plants10040792/s1>, Table S1: Protein quantification by nLC-nESI-MS/MS in M4 root proteome, Table S2: Functional classification of the identified proteins in M4 rootstock genotype.

Author Contributions: Conceptualization, B.P. and L.E.; methodology, B.P. and L.E.; investigation, B.P., C.M. and L.E.; validation, B.P., C.M. and L.E.; formal analysis, C.M. and B.P.; supervision, L.E.; writing—original draft preparation, L.E.; writing—review and editing, B.P. and L.E. All authors have read and agreed to the published version of the manuscript.

Funding: This research received no external funding.

Institutional Review Board Statement: Not applicable.

Informed Consent Statement: Not applicable.

Data Availability Statement: The data presented in this study are available on request from the corresponding author. The mass spectrometry proteomics data are available via ProteomeXchange with identifier PXD025212.

Acknowledgments: The authors thank colleagues Lucio Brancadoro for procuring the experimental material and Silvia Morgutti for reading through the manuscript.

Conflicts of Interest: The authors declare no conflict of interest.

References

- Hawkesford, M.; Horst, W.; Kichey, T.; Lambers, H.; Schjoerring, J.; Möller, I.S.; White, P. Chapter 6-Functions of Macronutrients. In *Marschner's Mineral Nutrition of Higher Plants*, 3rd ed.; Marschner, P., Ed.; Academic Press: San Diego, CA, USA, 2012; pp. 135–189. [\[CrossRef\]](#)
- Keller, M. *The Science of Grapevines: Anatomy and Physiology*, 2nd ed.; Keller, M., Ed.; Academic Press: Boston, MA, USA, 2015; ISBN 978-0-12-419987-3.
- Keller, M.; Kummer, M.; Vasconcelos, M.C. Reproductive Growth of Grapevines in Response to Nitrogen Supply and Rootstock. *Aust. J. Grape Wine Res.* **2001**, *7*, 12–18. [\[CrossRef\]](#)
- Bell, S.-J.; Henschke, P.A. Implications of Nitrogen Nutrition for Grapes, Fermentation and Wine. *Aust. J. Grape Wine Res.* **2005**, *11*, 242–295. [\[CrossRef\]](#)
- Gachons, C.P.; Leeuwen, C.V.; Tominaga, T.; Soyer, J.-P.; Gaudillère, J.-P.; Dubourdieu, D. Influence of Water and Nitrogen Deficit on Fruit Ripening and Aroma Potential of *Vitis vinifera* L. cv Sauvignon Blanc in Field Conditions. *J. Sci. Food Agr.* **2005**, *85*, 73–85. [\[CrossRef\]](#)
- Soubeyrand, E.; Basteau, C.; Hilbert, G.; van Leeuwen, C.; Delrot, S.; Gomès, E. Nitrogen Supply Affects Anthocyanin Biosynthetic and Regulatory Genes in Grapevine cv. Cabernet-Sauvignon Berries. *Phytochemistry* **2014**, *103*, 38–49. [\[CrossRef\]](#) [\[PubMed\]](#)
- Lecourt, J.; Lauvergeat, V.; Ollat, N.; Vivin, P.; Cookson, S.J. Shoot and Root Ionome Responses to Nitrate Supply in Grafted Grapevines Are Rootstock Genotype Dependent. *Aust. J. Grape Wine Res.* **2015**, *21*, 311–318. [\[CrossRef\]](#)
- Habran, A.; Commisso, M.; Helwi, P.; Hilbert, G.; Negri, S.; Ollat, N.; Gomès, E.; van Leeuwen, C.; Guzzo, F.; Delrot, S. Rootstocks/Scion/Nitrogen Interactions Affect Secondary Metabolism in the Grape Berry. *Front. Plant Sci.* **2016**, *7*. [\[CrossRef\]](#) [\[PubMed\]](#)
- Rosdeutscher, L.; Schreiner, R.P.; Skinkis, P.A.; Deluc, L. Nitrate Uptake and Transport Properties of Two Grapevine Rootstocks with Varying Vigor. *Front. Plant Sci.* **2021**, *11*. [\[CrossRef\]](#)
- Zapata, C.; Deléens, E.; Chaillou, S.; Magné, C. Partitioning and Mobilization of Starch and N Reserves in Grapevine (*Vitis Vinifera* L.). *J. Plant Physiol.* **2004**, *161*, 1031–1040. [\[CrossRef\]](#)
- Grechi, I.; Vivin, P.H.; Hilbert, G.; Milin, S.; Robert, T.; Gaudillère, J.-P. Effect of Light and Nitrogen Supply on Internal C:N Balance and Control of Root-to-Shoot Biomass Allocation in Grapevine. *Environ. Exp. Bot.* **2007**, *59*, 139–149. [\[CrossRef\]](#)
- Metay, A.; Magnier, J.; Guilpart, N.; Christophe, A. Nitrogen Supply Controls Vegetative Growth, Biomass and Nitrogen Allocation for Grapevine (cv. Shiraz) Grown in Pots. *Funct. Plant Biol.* **2015**, *42*, 105–114. [\[CrossRef\]](#)
- Ferrara, G.; Malerba, A.D.; Matarrese, A.M.S.; Mondelli, D.; Mazzeo, A. Nitrogen Distribution in Annual Growth of 'Italia' Table Grape Vines. *Front. Plant Sci.* **2018**, *9*. [\[CrossRef\]](#) [\[PubMed\]](#)
- Vrignon-Brenas, S.; Aurélie, M.; Romain, L.; Shiva, G.; Alana, F.; Myriam, D.; Gaëlle, R.; Anne, P. Gradual Responses of Grapevine Yield Components and Carbon Status to Nitrogen Supply. *OENO One* **2019**. [\[CrossRef\]](#)
- Jiménez, S.; Gogorcena, Y.; Hévin, C.; Rombolà, A.D.; Ollat, N. Nitrogen Nutrition Influences Some Biochemical Responses to Iron Deficiency in Tolerant and Sensitive Genotypes of *Vitis*. *Plant Soil* **2007**, *290*, 343–355. [\[CrossRef\]](#)
- Kulmann, M.S.; Sete, P.B.; Paula, B.V.; Stefanello, L.O.; Schwalbert, R.; Schwalbert, R.A.; Arruda, W.S.; Sans, G.A.; Parciannelo, C.F.; Nicoloso, F.T.; et al. Kinetic Parameters Govern the Uptake of Nitrogen Forms in 'Paulsen' and 'Magnolia' Grapevine Rootstocks. *Sci. Hortic.* **2020**, *264*, 109174. [\[CrossRef\]](#)
- Miller, A.J.; Fan, X.; Orsel, M.; Smith, S.J.; Wells, D.M. Nitrate Transport and Signalling. *J. Exp. Bot.* **2007**, *58*, 2297–2306. [\[CrossRef\]](#) [\[PubMed\]](#)
- Wang, Y.-Y.; Hsu, P.-K.; Tsay, Y.-F. Uptake, Allocation and Signaling of Nitrate. *Trends Plant Sci.* **2012**, *17*, 458–467. [\[CrossRef\]](#)
- Fan, X.; Naz, M.; Fan, X.; Xuan, W.; Miller, A.J.; Xu, G. Plant Nitrate Transporters: From Gene Function to Application. *J. Exp. Bot.* **2017**, *68*, 2463–2475. [\[CrossRef\]](#)
- Pii, Y.; Alessandrini, M.; Guardini, K.; Zamboni, A.; Varanini, Z. Induction of High-Affinity NO₃⁻ Uptake in Grapevine Roots Is an Active Process Correlated to the Expression of Specific Members of the NRT2 and Plasma Membrane H⁺-ATPase Gene Families. *Funct. Plant Biol.* **2014**, *41*, 353–365. [\[CrossRef\]](#)
- Tomasi, N.; Monte, R.; Varanini, Z.; Cesco, S.; Pinton, R. Induction of Nitrate Uptake in Sauvignon Blanc and Chardonnay Grapevines Depends on the Scion and Is Affected by the Rootstock. *Aust. J. Grape Wine Res.* **2015**, *21*, 331–338. [\[CrossRef\]](#)
- Loulakakis, K.A.; Morot-Gaudry, J.F.; Velanis, C.N.; Skopelitis, D.S.; Moschou, P.N.; Hirel, B.; Roubelakis-Angelakis, K.A. Advancements in Nitrogen Metabolism in Grapevine. In *Grapevine Molecular Physiology & Biotechnology*; Roubelakis-Angelakis, K.A., Ed.; Springer: Dordrecht, The Netherlands, 2009; pp. 161–205. [\[CrossRef\]](#)
- Zerihun, A.; Treeby, M.T. Biomass Distribution and Nitrate Assimilation in Response to N Supply for *Vitis vinifera* L. cv. Cabernet Sauvignon on Five *Vitis* Rootstock Genotypes. *Aust. J. Grape Wine Res.* **2002**, *8*, 157–162. [\[CrossRef\]](#)
- Lang, C.P.; Merkt, N.; Zörb, C. Different Nitrogen (N) Forms Affect Responses to N Form and N Supply of Rootstocks and Grafted Grapevines. *Plant Sci.* **2018**, *277*, 311–321. [\[CrossRef\]](#)
- Lang, C.P.; Bárdos, G.; Merkt, N.; Zörb, C. Expression of Key Enzymes for Nitrogen Assimilation in Grapevine Rootstock in Response to N-Form and Timing. *J. Plant Nutr. Soil Sci.* **2020**, *183*, 91–98. [\[CrossRef\]](#)

26. Scheible, W.-R.; Morcuende, R.; Czechowski, T.; Fritz, C.; Osuna, D.; Palacios-Rojas, N.; Schindelasch, D.; Thimm, O.; Udvardi, M.K.; Stitt, M. Genome-Wide Reprogramming of Primary and Secondary Metabolism, Protein Synthesis, Cellular Growth Processes, and the Regulatory Infrastructure of Arabidopsis in Response to Nitrogen. *Plant Physiol.* **2004**, *136*, 2483–2499. [\[CrossRef\]](#)
27. Nunes-Nesi, A.; Fernie, A.R.; Stitt, M. Metabolic and Signaling Aspects Underpinning the Regulation of Plant Carbon Nitrogen Interactions. *Mol. Plant* **2010**, *3*, 973–996. [\[CrossRef\]](#)
28. Cochetel, N.; Escudie, F.; Cookson, S.J.; Dai, Z.; Vivin, P.; Bert, P.-F.; Muñoz, M.S.; Delrot, S.; Klopp, C.; Ollat, N.; et al. Root Transcriptomic Responses of Grafted Grapevines to Heterogeneous Nitrogen Availability Depend on Rootstock Genotype. *J. Exp. Bot.* **2017**, *68*, 4339–4355. [\[CrossRef\]](#)
29. Wang, R.; Okamoto, M.; Xing, X.; Crawford, N.M. Microarray Analysis of the Nitrate Response in Arabidopsis Roots and Shoots Reveals over 1000 Rapidly Responding Genes and New Linkages to Glucose, Trehalose-6-Phosphate, Iron, and Sulfate Metabolism. *Plant Physiol.* **2003**, *132*, 556–567. [\[CrossRef\]](#) [\[PubMed\]](#)
30. Lejay, L.; Wirth, J.; Pervent, M.; Cross, J.M.-F.; Tillard, P.; Gojon, A. Oxidative Pentose Phosphate Pathway-Dependent Sugar Sensing as a Mechanism for Regulation of Root Ion Transporters by Photosynthesis. *Plant Physiol.* **2008**, *146*, 2036–2053. [\[CrossRef\]](#) [\[PubMed\]](#)
31. Meggio, F.; Prinsi, B.; Negri, A.S.; Lorenzo, G.S.D.; Lucchini, G.; Pitacco, A.; Failla, O.; Scienza, A.; Cocucci, M.; Espen, L. Biochemical and Physiological Responses of Two Grapevine Rootstock Genotypes to Drought and Salt Treatments. *Aust. J. Grape Wine Res.* **2014**, *20*, 310–323. [\[CrossRef\]](#)
32. Corso, M.; Vannozzi, A.; Maza, E.; Vitulo, N.; Meggio, F.; Pitacco, A.; Telatin, A.; D'Angelo, M.; Feltrin, E.; Negri, A.S.; et al. Comprehensive Transcript Profiling of Two Grapevine Rootstock Genotypes Contrasting in Drought Susceptibility Links the Phenylpropanoid Pathway to Enhanced Tolerance. *J. Exp. Bot.* **2015**, *66*, 5739–5752. [\[CrossRef\]](#)
33. Prinsi, B.; Negri, A.S.; Failla, O.; Scienza, A.; Espen, L. Root Proteomic and Metabolic Analyses Reveal Specific Responses to Drought Stress in Differently Tolerant Grapevine Rootstocks. *BMC Plant Biol.* **2018**, *18*, 126. [\[CrossRef\]](#) [\[PubMed\]](#)
34. Prinsi, B.; Failla, O.; Scienza, A.; Espen, L. Root Proteomic Analysis of Two Grapevine Rootstock Genotypes Showing Different Susceptibility to Salt Stress. *Int. J. Mol. Sci.* **2020**, *21*, 1076. [\[CrossRef\]](#)
35. Prinsi, B.; Simeoni, F.; Galbiati, M.; Meggio, F.; Tonelli, C.; Scienza, A.; Espen, L. Grapevine Rootstocks Differently Affect Physiological and Molecular Responses of the Scion under Water Deficit Condition. *Agronomy* **2021**, *11*, 289. [\[CrossRef\]](#)
36. Xu, G.; Fan, X.; Miller, A.J. Plant Nitrogen Assimilation and Use Efficiency. *Annu. Rev. Plant Biol.* **2012**, *63*, 153–182. [\[CrossRef\]](#) [\[PubMed\]](#)
37. Gilmore, J.M.; Washburn, M.P. Advances in Shotgun Proteomics and the Analysis of Membrane Proteomes. *J. Proteom.* **2010**, *73*, 2078–2091. [\[CrossRef\]](#)
38. Schwacke, R.; Ponce-Soto, G.Y.; Krause, K.; Bolger, A.M.; Arsova, B.; Hallab, A.; Gruden, K.; Stitt, M.; Bolger, M.E.; Usadel, B. MapMan4: A Refined Protein Classification and Annotation Framework Applicable to Multi-Omics Data Analysis. *Mol. Plant* **2019**, *12*, 879–892. [\[CrossRef\]](#) [\[PubMed\]](#)
39. Canales, J.; Moyano, T.C.; Villarreal, E.; Gutiérrez, R.A. Systems Analysis of Transcriptome Data Provides New Hypotheses about Arabidopsis Root Response to Nitrate Treatments. *Front. Plant Sci.* **2014**, *5*. [\[CrossRef\]](#)
40. Prinsi, B.; Espen, L. Time-Course of Metabolic and Proteomic Responses to Different Nitrate/Ammonium Availabilities in Roots and Leaves of Maize. *Int. J. Mol. Sci.* **2018**, *19*, 2202. [\[CrossRef\]](#)
41. Bernard, S.M.; Habash, D.Z. The Importance of Cytosolic Glutamine Synthetase in Nitrogen Assimilation and Recycling. *New Phytol.* **2009**, *182*, 608–620. [\[CrossRef\]](#)
42. Stitt, M. Nitrate Regulation of Metabolism and Growth. *Curr. Opin. Plant Biol.* **1999**, *2*, 178–186. [\[CrossRef\]](#)
43. Stein, O.; Granot, D. An Overview of Sucrose Synthases in Plants. *Front. Plant Sci.* **2019**, *10*. [\[CrossRef\]](#)
44. Sun, J.-L.; Li, J.-Y.; Wang, M.-J.; Song, Z.-T.; Liu, J.-X. Protein Quality Control in Plant Organelles: Current Progress and Future Perspectives. *Mol. Plant* **2021**, *14*, 95–114. [\[CrossRef\]](#) [\[PubMed\]](#)
45. Kohli, A.; Narciso, J.O.; Miro, B.; Raorane, M. Root Proteases: Reinforced Links between Nitrogen Uptake and Mobilization and Drought Tolerance. *Physiol. Plant.* **2012**, *145*, 165–179. [\[CrossRef\]](#)
46. Wang, Y.-H.; Garvin, D.F.; Kochian, L.V. Nitrate-Induced Genes in Tomato Roots. Array Analysis Reveals Novel Genes That May Play a Role in Nitrogen Nutrition. *Plant Physiol.* **2001**, *127*, 345–359. [\[CrossRef\]](#) [\[PubMed\]](#)
47. Park, S.-C.; Kim, Y.-H.; Jeong, J.C.; Kim, C.Y.; Lee, H.-S.; Bang, J.-W.; Kwak, S.-S. Sweetpotato Late Embryogenesis Abundant 14 (IbLEA14) Gene Influences Lignification and Increases Osmotic- and Salt Stress-Tolerance of Transgenic Calli. *Planta* **2011**, *233*, 621–634. [\[CrossRef\]](#)
48. Yu, P.; Li, X.; Yuan, L.; Li, C. A Novel Morphological Response of Maize (*Zea mays*) Adult Roots to Heterogeneous Nitrate Supply Revealed by a Split-Root Experiment. *Physiol. Plant.* **2014**, *150*, 133–144. [\[CrossRef\]](#)
49. Vega, A.; O'Brien, J.A.; Gutiérrez, R.A. Nitrate and Hormonal Signaling Crosstalk for Plant Growth and Development. *Curr. Opin. Plant Biol.* **2019**, *52*, 155–163. [\[CrossRef\]](#) [\[PubMed\]](#)
50. Kose, C.; Erdal, S.; Kaya, O.; Atici, O. Comparative Evaluation of Oxidative Enzyme Activities during Adventitious Rooting in the Cuttings of Grapevine Rootstocks. *J. Sci. Food Agr.* **2011**, *91*, 738–741. [\[CrossRef\]](#)
51. Fritz, C.; Palacios-Rojas, N.; Feil, R.; Stitt, M. Regulation of Secondary Metabolism by the Carbon–Nitrogen Status in Tobacco: Nitrate Inhibits Large Sectors of Phenylpropanoid Metabolism. *Plant J.* **2006**, *46*, 533–548. [\[CrossRef\]](#)

52. He, F.; Mu, L.; Yan, G.-L.; Liang, N.-N.; Pan, Q.-H.; Wang, J.; Reeves, M.J.; Duan, C.-Q. Biosynthesis of Anthocyanins and Their Regulation in Colored Grapes. *Molecules* **2010**, *15*, 9057–9091. [[CrossRef](#)]
53. Larbat, R.; Bot, J.L.; Bourgaud, F.; Robin, C.; Adamowicz, S. Organ-Specific Responses of Tomato Growth and Phenolic Metabolism to Nitrate Limitation. *Plant Biol.* **2012**, *14*, 760–769. [[CrossRef](#)]
54. Prinsi, B.; Negrini, N.; Morgutti, S.; Espen, L. Nitrogen Starvation and Nitrate or Ammonium Availability Differently Affect Phenolic Composition in Green and Purple Basil. *Agronomy* **2020**, *10*, 498. [[CrossRef](#)]
55. Schmidlin, L.; Poutaraud, A.; Claudel, P.; Mestre, P.; Prado, E.; Santos-Rosa, M.; Wiedemann-Merdinoglu, S.; Karst, F.; Merdinoglu, D.; Hugueney, P. A Stress-Inducible Resveratrol O-Methyltransferase Involved in the Biosynthesis of Pterostilbene in Grapevine. *Plant Physiol.* **2008**, *148*, 1630–1639. [[CrossRef](#)]
56. Ramawat, K.G.; Goyal, S. Co-Evolution of Secondary Metabolites During Biological Competition for Survival and Advantage: An Overview. In *Co-Evolution of Secondary Metabolites*; Merillon, J.-M., Ramawat, K.G., Eds.; Reference Series in Phytochemistry; Springer International Publishing: Cham, Germany, 2019; pp. 1–15. [[CrossRef](#)]
57. González, J.F.; Venturi, V. A Novel Widespread Interkingdom Signaling Circuit. *Trends Plant Sci.* **2013**, *18*, 167–174. [[CrossRef](#)]
58. Di, C.; Xu, W.; Su, Z.; Yuan, J.S. Comparative Genome Analysis of PHB Gene Family Reveals Deep Evolutionary Origins and Diverse Gene Function. *BMC Bioinform.* **2010**, *11*, S22. [[CrossRef](#)]
59. Wang, Y.; Yang, L.; Chen, X.; Ye, T.; Zhong, B.; Liu, R.; Wu, Y.; Chan, Z. Major Latex Protein-like Protein 43 (MLP43) Functions as a Positive Regulator during Absciscic Acid Responses and Confers Drought Tolerance in *Arabidopsis thaliana*. *J. Exp. Bot.* **2016**, *67*, 421–434. [[CrossRef](#)]
60. Konopka-Postupolska, D.; Clark, G.; Hofmann, A. Structure, Function and Membrane Interactions of Plant Annexins: An Update. *Plant Sci.* **2011**, *181*, 230–241. [[CrossRef](#)]
61. Yoo, K.S.; Ok, S.H.; Jeong, B.-C.; Jung, K.W.; Cui, M.H.; Hyoun, S.; Lee, M.-R.; Song, H.K.; Shin, J.S. Single Cystathionine β -Synthase Domain-Containing Proteins Modulate Development by Regulating the Thioredoxin System in Arabidopsis. *Plant Cell* **2011**, *23*, 3577–3594. [[CrossRef](#)] [[PubMed](#)]
62. Noctor, G.; Mhamdi, A.; Chaouch, S.; Han, Y.; Neukermans, J.; Marquez-Garcia, B.; Queval, G.; Foyer, C.H. Glutathione in Plants: An Integrated Overview. *Plant Cell Environ.* **2012**, *35*, 454–484. [[CrossRef](#)] [[PubMed](#)]
63. Cataldo, D.A.; Maroon, M.; Schrader, L.E.; Youngs, V.L. Rapid Colorimetric Determination of Nitrate in Plant Tissue by Nitration of Salicylic Acid. *Commun. Soil Sci. Plant* **1975**, *6*, 71–80. [[CrossRef](#)]
64. Moore, S.; Stein, W.H. A Modified Ninhydrin Reagent for the Photometric Determination of Amino Acids and Related Compounds. *J. Biol. Chem.* **1954**, *211*, 907–913. [[CrossRef](#)]
65. Nelson, N. A Photometric Adaptation of the Somogyi Method for the Determination of Glucose. *J. Biol. Chem.* **1944**, *153*, 375–380. [[CrossRef](#)]
66. Prinsi, B.; Negri, A.S.; Pesaresi, P.; Cocucci, M.; Espen, L. Evaluation of Protein Pattern Changes in Roots and Leaves of *Zea mays* plants in Response to Nitrate Availability by Two-Dimensional Gel Electrophoresis Analysis. *BMC Plant Biol.* **2009**, *9*, 113. [[CrossRef](#)]
67. Laemmli, U.K. Cleavage of Structural Proteins during the Assembly of the Head of Bacteriophage T4. *Nature* **1970**, *227*, 680–685. [[CrossRef](#)] [[PubMed](#)]
68. Vizcaíno, J.A.; Deutsch, E.W.; Wang, R.; Csordas, A.; Reisinger, F.; Ríos, D.; Dianes, J.A.; Sun, Z.; Farrah, T.; Bandeira, N.; et al. ProteomeXchange Provides Globally Co-Ordinated Proteomics Data Submission and Dissemination. *Nat. Biotechnol.* **2014**, *32*, 223–226. [[CrossRef](#)] [[PubMed](#)]